SPE-187495-MS

Development of an Empirical Equation to Predict Hydraulic Fracture Closure Pressure from the Initial Shut-in Pressure after Treatment

S. M. Kholy, I. M. Mohamed, M. Loloi, O. Abou-Sayed, and A. Abou-Sayed, Advantek Waste Management Services

This paper was prepared for presentation at the SPE Liquids-Rich Basins Conference - North America held in Midland, Texas, USA, 13-14 September 2017.

Abstract

During hydraulic fracturing operations, conventional pressure fall-off analyses (G-Function, Square Root of Time, and Diagnostic Plots) are the main methods for predicting fracture closure pressure. However, there are situations when it is not practical to determine the fracture closure pressure using these analyses. These conditions occur when closure time is long, such as in mini-frac tests in very tight formations, or waste fluid injection in reservoirs where there is low native permeability or where there is significant near wellbore damage. In these situations, it can take several days for the shut-in pressure to stabilize enough for conventional pressure fall-off tests analyses to be used. Thus, the objective of the present study is to attempt to correlate the fracture closure pressure to the early time fall off data using the field-measured Initial Shut-in Pressure (ISIP), rock properties and pumped / injection volumes.

A study of the injection pressure history of many injection wells with multiple hydraulic fractures in a variety of rock lithologies shows an interesting relationship between the fracture closure pressure and the initial shut-in pressure. An empirical equation has been created to calculate the fracture closure pressure as a function of the instantaneous shut-in pressure (ISIP) and the injection formation rock properties. Such rock properties include formation permeability, formation porosity, reservoir pressure, overburden pressure, Poisson's ratio, and Young's modulus. An empirical equation was developed using the injected volumes combined with data obtained from geomechancial models and core analysis of a wide range of injection horizons in terms of lithology type: Sandstone, Carbonate, and Shale.

The empirical equation was validated using different case studies by comparing the predicted fracture closure pressure calculated using the developed empirical equation to the measured fracture closure pressure value. The reported correlation predicted the fracture closure pressure with a relative error of less than 6%. Also, the empirical equation was used to predict the fracture closure pressure in a shale formation with less than 3% error.

The new empirical equation predicts the fracture closure pressure using a single point of falloff pressure data, the ISIP, without the need to conduct a conventional fracture closure analysis. This allows the operator to avoid having to collect pressure data between shut-in and until the actual fracture closure point which can take several days in highly damaged, very tight, and/or shale formations. Moreover, in operations with multiple batch injection events into the same interval / perforations, as is often found cuttings / slurry

injection operations, the trends in closure pressure evolution can be tracked even if the fracture is never allowed to close.

Introduction

Hydraulic fracturing was first used in 1949 to stimulate reservoirs and improve hydroncarbon recovery (Gandossi et al. 2015). It involves creating a fracture in the desired subsurface formation by injecting clean water downhole the well at a pressure higher than the formation minimum stress (Kiel 1970). Later in the 1980s, hydraulic fracturing has been widely used in many oilfield applications, such as: well stimulation, sand control, and oilfield waste fractured injection.

As for well stimulation, the created fracture is filled by proppant to keep the fracture open and eventually to enhance well production rates (Warembourg et al. 1985). Frac-Pack is another application which is used to control sand production for unconsolidated sand reservoirs (Tiner et al. 1996). Moreover, Hydraulic fracturing results in many other injection operations, for example: water flooding, enhanced oil recovery (EOR) and waste injection. In the later example, hydraulic fracturing creates underground channels to assists in re-injection of slurrified wastes. This technique ensures environmentally safe disposal of wastes within a created secure subsurface storage domain (Moschovidis et al. 1999; Abou-Sayed et al. 1989; and Sirevag et al. 1993).

Each of these applications requires good knowledge about the properties of the created fracture, for example; facture dimensions, fracture closure, and fracture propagation in order to conduct the specific operations successfully. One of the key formation properties is the formation fracture pressure, which is essential for selecting the proper pumps to create a hydraulic fracture (Fast et al. 1970). There are several techniques to estimate the fracture pressure using predictive and analytical methods. Predictive methods are used to estimate the fracture pressure by developing empirical equations based on the formation geophysical properties, overburden pressure, and pore pressure (Hubbert and Willis 1957, Mathews and Kelly 1967; and Eaton 1969). On the other hand, analytical methods are used to estimate the fracture pressure during or after running an inejction test (Nolte 1979, Singh et al. 1987, Barree et al. 2009; and Mohamed et al. 2011). Also, analytical methods are used to monitor the fracture pressure development as the in-situ stresses re-orient and reservoir properties change over time (Perkins and Gonzalez 1985; Warpinski and Branagan 1989).

These after-treatment analytical methods require monitoring of the shut-in pressure data to identify the transition from linear flow (fracture flow) to radial flow (matrix flow) regimes. However, the fracture closure time may extend for days when the fluid leakoff rate is extremely slow, especially in very tight formations (shales or ultra low-permeability sands) or wells with significant near wellbore damage. Therefore, a new empirical equation was developed to speed the process of estimating the fracture closure pressure right after injection stops and the well is shut-in instead of waiting for the fracture to close. The input data for this new empirical equation include petrophysical and mechaical properties (porosity, permeability, Young's modulus, and Poisson's Ratio) while only one pressure fall off data point is needed, the Instantaneous Shut-In Pressure (ISIP).

Review of Existing Predictive Methods

Hubbert and Willis Equation:. (Hubbert and Willis 1957) have developed the first correlation for fracture pressure prediction. They found that the fracture pressure, P_w, is a function of overburden stress, a, formation pore pressure, P, and horizontal-to-vertical stress ratio, K_i which has been considered to be constant with depth at a value of one-third as shown in Eq. 1:

$$\frac{P_w}{D} = \left(1.0 + \frac{2P}{D}\right).\left(\frac{1}{3}\right) \quad (1)$$

Matthews and Kelly Equation:. (Matthews and Kelly 1967) introduced a new term (borrowed from soil mechanics and called matrix stress coefficient K_i) that accounts for the effect of depth on the horizontal-to-vertical stress ratio as shown by Eq. 2:

$$\frac{P_w}{D} = K_i\left(\frac{\sigma}{D} + \frac{P}{D}\right) \quad (2)$$

Eaton Equation:. Eaton (1969; 1975) addressed the effect of overburden gradient, poisson's ratio, and pore pressure gradient on Eq. 1.

Analytical Methods

Step Rate Test Analysis:. (Felsenthal 1974) proposed new injection test procedures which involve injecting water into the desired formation in steps with different injection flow rate. Each injection flow rate is kept constant until the injection pressure stabilizes, then the flow rate is stepped up to a higher flow rate and so on. The recorded stabilized pressure values are plotted versus the corresponding flow rates so that the fracture pressure represents the intersection point oftwo straight lines with different slopes indicating transition from matrix flow to fracture flow. However, the intersection point is found to be higher than the actual fracture pressure due to the additional friction losses across both the tubing and the perforated interval during the injection. Upon the transition to fracture flow, the fracture growth can be monitored with time following the analysis procedures by (Singh et al. 1987).

G-Function Analysis:. The G-function analysis, introduced by Nolte (1979), uses a time function to estimate the fracture closure time and reservoir permeability. This technique is considered a pre-closure analysis of the falloff test, and is dependent on pressure leakoff rate.

The equations below to calculate the G-function:

$$\Delta t_D = \left(\frac{t - t_p}{t_p}\right) \quad (3)$$

$$g(\Delta t_D) = \frac{4}{3}\left[(1 + \Delta t_D)^{1.5} - \Delta t_D^{1.5}\right] \quad (4)$$

$$G(\Delta t_D) = \frac{4}{\pi}\left(g(\Delta t_D) - g_o\right) \quad (5)$$

(Barree et al. 2009) suggested that the fracture closure represents the departure of the derivative from the straight line through the origin and tangent to the derivative curve.

Square Root of Time Analysis:. (Howard et al.1957) introduced a method to determine the fracture pressure by ploting the fall off pressure versus the square root of shut-in time so that the fracture closure is identified when the declining pressure starts to deviate from linearity. Later, (Barree et al. 2009) suggested that the fracture closure can be determined from plotting the pressure derivative with respect to square root of time versus the square root of time and the departure of the derivative form the straight line represents the fracture closure.

Log-Log Diagnostic Plot Analysis:. The log-log diagnostic plot of pressure drop and its logarithmic derivative is a conventional method used to interpret any transient well test. The logarithmic derivative is computed as the derivative of the pressure with respect to the logarithm of superposition time $\left(\frac{t+t_p}{t_p}\right)$. The pressure derivative shows different characteristic slopes, each of which can be interpreted as a specific flow regime. Radial flow represents flat line of zero slope, linear flow is representd by a half-slope line, and the bilinear flow is represented by aquarter-slope line. (Mohamed et al. 2011) showed that the fracture closure can be picked from the log-log diagnostic plot when the logarithmic pressure derivative leaves the 3/2 slope.

Field Observations

Advantek Waste Management Services drilled and completed the Reed well, located in South Texas, USA, down to the Wilcox formation in order to serve as an Underground Injection Contol (UIC) Class II waste injector. In general, UIC Class II wells are used for downhole injection of all types of non- hazardous (exempt) waste such as oil-based mud, water-based mud, drill cuttings, and oily prudced water that are produced by drilling and production operations from surrounding wells. Based on waste injection best practices, the waste injection is conducted in cycles so that a fracture is initiated hydraulically by clean water then the waste is injected downhole to fill and to propagate the hydraulic fracture. Finally, the well is shut-in so that the created fracture heals and closes off, allowing near wellbore stresses to reorient, before starting a new batch injection.

After each batch injection, the ISIP is picked manually as shown in (Fig. 1) which represents the final downhole injection pressure minus the friction losses in the tubing and along the fracture (Mclennan et al. 1982). On the other hand, the fracture closure pressure is determined by analyzing the fall-off data after following batch injection, using G-function analysis as shown in (Fig. 2). Hence, both the fracture closure pressure and the ISIP are recorded based on the batch to batch pressure post-shut-in analysis.

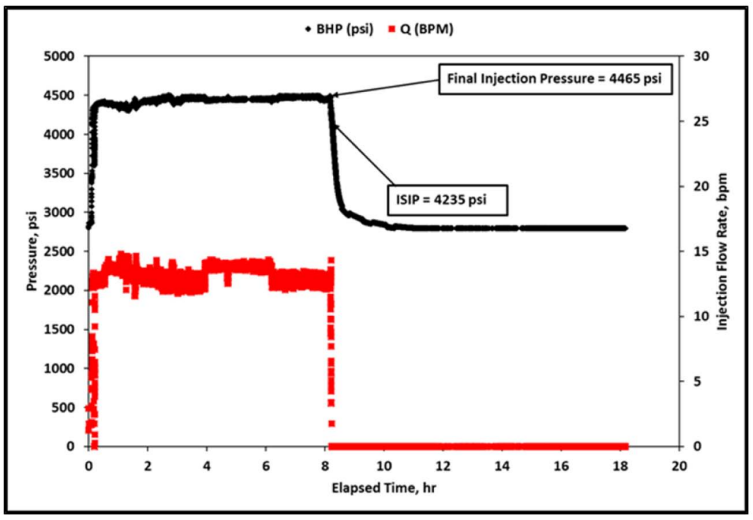

Figure 1—Injection Pressure and Injection Flow Rate Data for Reed Well

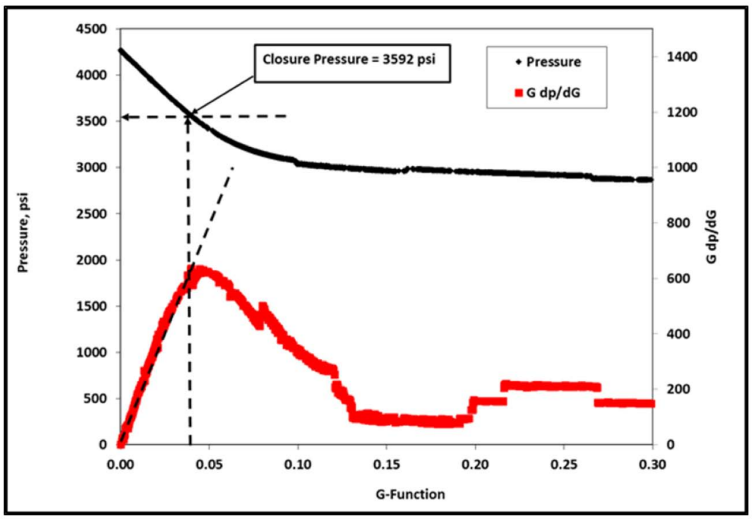

Figure 2—Fracture Closure Pressure from G-Function Analysis for Reed Well

The injection history (Fig. 3) of the Reed well demonstrates a clear correlation between the ISIP and the fracture closure pressure (Pc) for that well. Hence, (Fig. 4) shows a linear relationship for the Reed Well between ISIP and Pc was obtained as shown by Eq. 8:

$$P_C = C_1.ISIP + C_2 \tag{6}$$

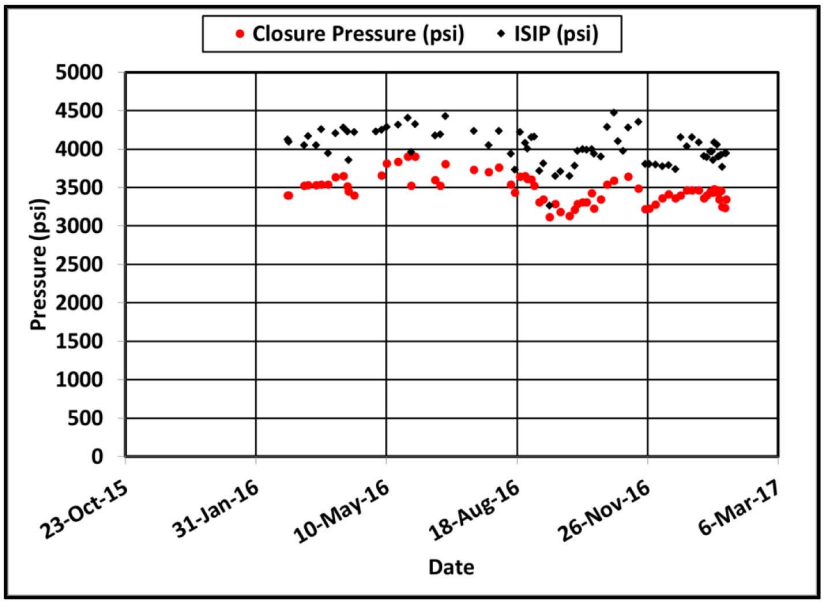

Figure 3—Fracture Closure Pressure and ISIP History for Reed Well

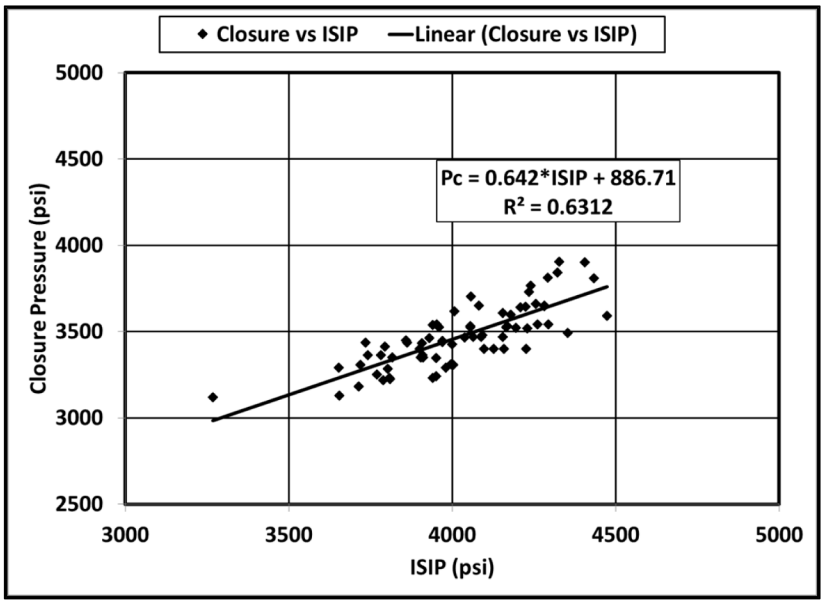

Figure 4—Fitting Fracture Closure Pressure with ISIP for Reed Well

Where:

C_1 and C_2, the linear regression coefficients, are functions of the formation and injection variables.

The same procedures were used to obtain the relationship between closure pressure and ISIP for four other injectors with different lithologies, reservoir properties, mechanical properties, and depths. The results confirm the linear relationship between ISIP and closure pressure for a variety of batch volumes. The linear regression coefficients for each well are summarized in Table 1.

Table 1—Linear regression coefficients for different Injectors

Well Name	Injection Formation Lithology	C_1	C_2
Reed	Consolidated Sand with interbedded Shale	0.642	886.71
A	Limestone	0.5929	1061.6
B	Iimestone with interbedded Dolomite	0.7422	589.36
C	Unconsolidated Sandstone	0.2752	302.44
D	Sandstone	0.6335	118.79

A New Technique

To develop a generalized equation applicable across various lithologies, a generic form for the linear coefficients C_1 and C_2 in Eq. 6 to estimate the fracture closure pressure from ISIP must be created. The generalized equation is developed in four steps as described below:

1. Collect reservoir properties for the available wells
2. Test which property is is closely related to C_1 and which property C_2 is sensitive to. Eliminate all the correlations with a fitting error ($R^2 \leq 0.5$)
3. Combine the correlations from step 2 to get the generic forms for C_1 and C_2
4. Finally, calcute the absolute error in estimating the constants C1 and C2.

A more detailed description of these four steps follows.

Step (1): Measure and calculate the reservoir properties for the representative wells

Formation Porosity. Formation porosity was obtained from the side wall cores collected from Wilcox formation. The average formation porosity is 17%.

Pore Pressure and Overburden Pressure. Sonic logs were used to predict the formation pore pressure (2400 psi) using the equation developed by Eaton (1975). On the other hand, the overburden pressure was determined from bulk density logs (6000 psi).

Formation Permeability. The formation permeability can be determined from the radial flow regime. The radial flow is defined by a zero-slope line on the pressure derivative curve in the log-log diagnostic plot and exists in the time period before the pressure transient has reached the reservoir boundaries. (Horner 1951) developed Eq. 7 in order to calculate the permeability:

$$K = \frac{70.6qB\mu}{m'h} \tag{7}$$

(Fig. 5) shows that *m'* equals to 96 for Reed well and, therefore, the Wilcox permeability is 70 mD.

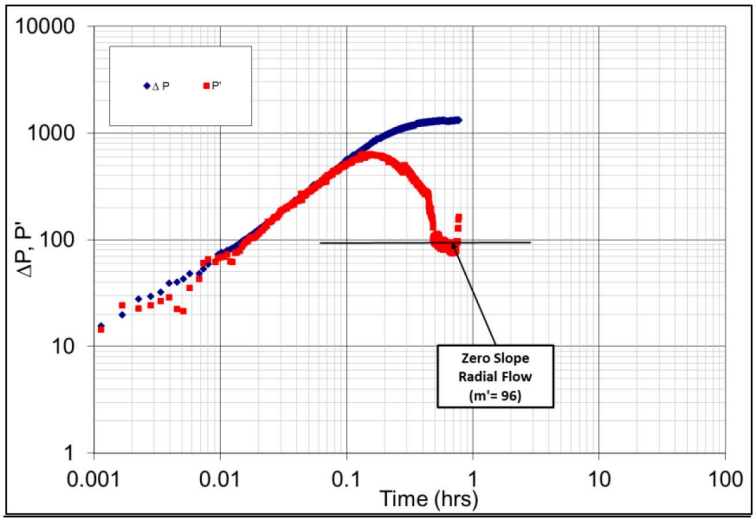

Figure 5—Log-Log Diagnostic Plot for Reed Well

Poisson 's Ratio. Poisson's ratio was calculated from the sonic logs (Fig. 6), using the following equation:

$$\upsilon = \frac{0.5\frac{V_p^2}{V_s^2}-1}{\frac{V_p^2}{V_s^2}-1} \tag{8}$$

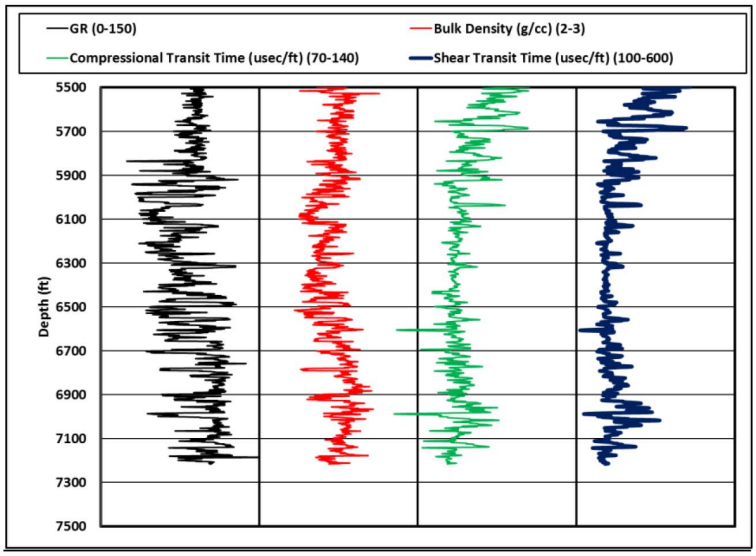

Figure 6—Well Logs for Reed Well

Young's Modulus. Canady (2011) developed a formula to calculate the static Young's modulus from the dynamic modulus as shown by Eq. 9:

$$E_s = \frac{ln(E_d+1).(E_d-2)}{4.5} \tag{9}$$

Where:

$$E_d = 2\rho V_s^2(1+\upsilon)$$

(Fig. 7) shows the calculated reservoir properties for Reed well. Table 2 summarizes the reservoir properties for all five wells.

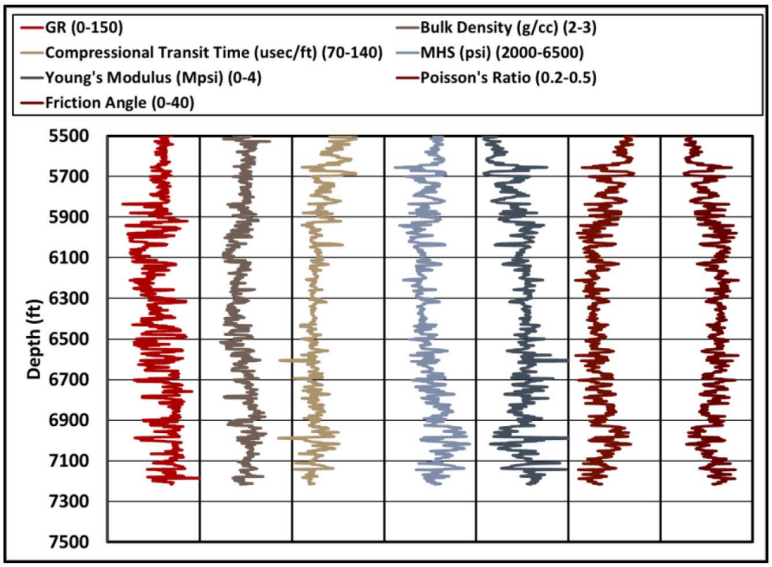

Figure 7—Mechanical Properties Calculations for Reed Well

Table 2—Summary of the reservoir properties for the five wells

Well Name	Permeability (mD)	Young's Modulus (Mpsi)	Porosity (fraction)	Poisson's Ratio	Pore Pressure (psi)	Overburden Pressure (psi)
Reed	70	2.3	0.17	0.3	2400	6000
A	65	2.4	0.17	0.33	2370	4644
B	30	2	0.22	0.29	2411	4887
C	180	0.52	0.19	0.28	365	1225
D	70	0.49	0.22	0.22	413	1339

Step (2): Plot each reservoir property versus C_1 and C_2 and eliminate all the correlations with a fitting error ($R^2 \leq 0.5$)

C_1 and C_2 were separately plotted versus each of the measured reservoir properties mentioned in Table 2. The results show that C_1 is a function of formation permeability while C_2 is a function of porosity, pore pressure, overburden pressure, Poisson's ratio and Young's Modulus as shown in (Fig. 8-13).

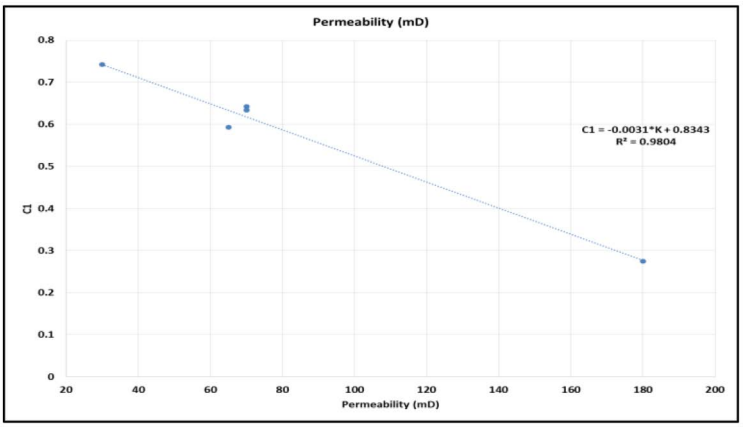

Figure 8—C_1 versus Permeability

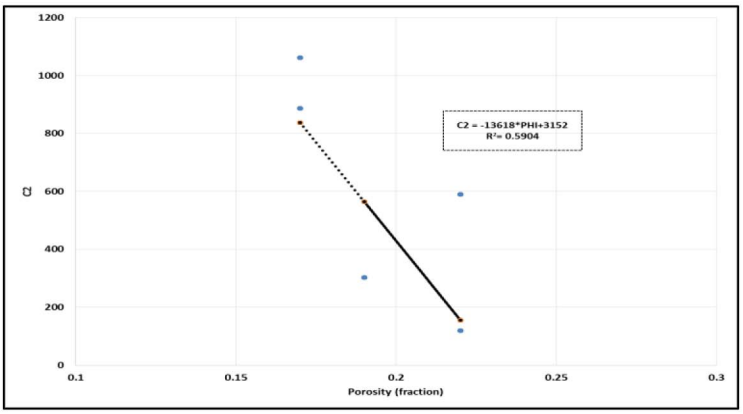

Figure 9—C_2 versus Porosity

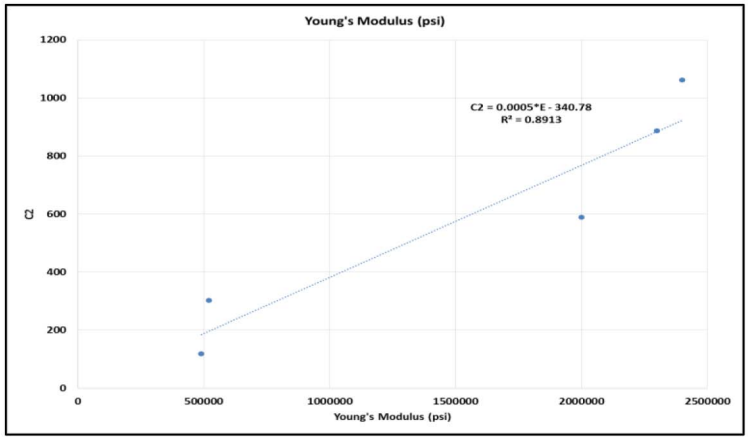

Figure 10—C_2 versus Young's Modulus

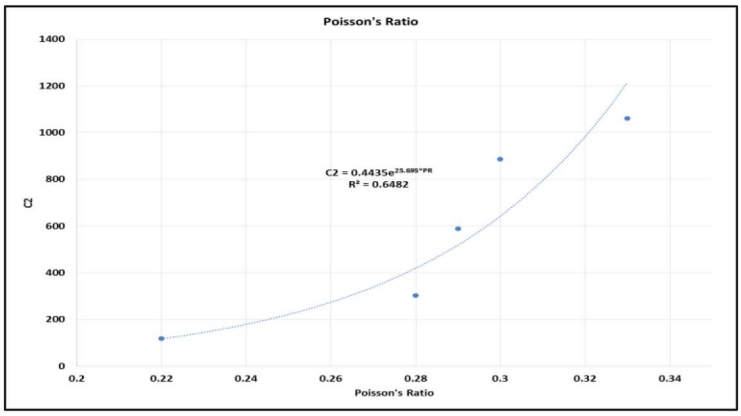

Figure 11—C_2 versus Poisson's Ratio

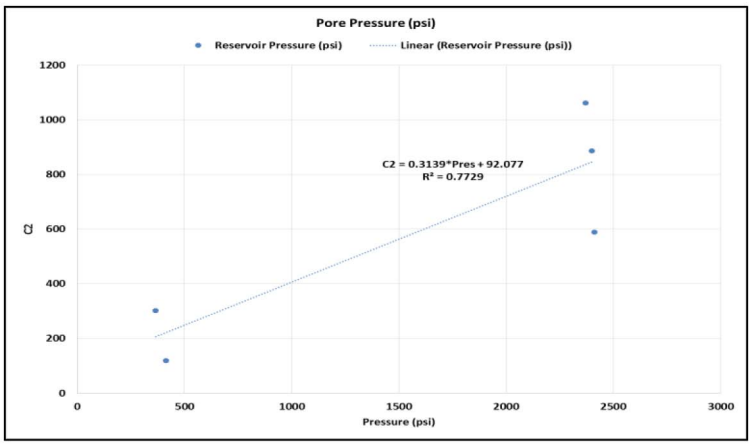

Figure 12—C_2 versus Pore Pressure

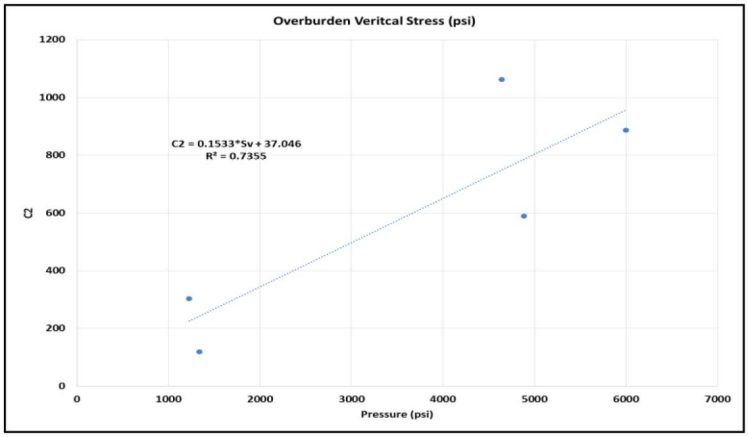

Figure 13—C_2 versus Overburden Pressure

Step (3): Combine the correlations from step 2 to get the generic forms for C_1 and C_2

The acceptable correlations from step 2 are combined together to produce the generic forms for C1 and C2 as in Eq. 10 and Eq. 11:

$$C_1 = C_{1,K} \tag{10}$$

$$C_2 = \frac{\left(C_{2,E}+C_{2,\upsilon}+C_{2,P}+C_{2,S}+C_{2,\phi}\right)}{5} \tag{11}$$

Where:

$$C_{1,K} = -0.0031K + 0.8343 \qquad C_{2,P} = 0.3139P + 92.077$$

$$C_{2,E} = 0.00005E + 340.78 \qquad C_{2,S} = 0.1533S + 37.046$$

$$C_{2,\upsilon} = 0.4435EXP(25.695\upsilon) \qquad C_{2,\phi} = -13618\phi + 3152$$

Step (4): Compare C1 and C2 from the new formulae to the original values

Table 3 summarizes the original values of C_1 and C_2 obtained from the linear fitting of injection history data for each of the five wells, and the calculated values from the new formulae. (Fig. 14) shows a comparison between the fracture closure pressure from the G-function analysis and from the new empirical equation for Reed well which indicates a relative error of 3%. The discrepancies are due to the different levels of uncertainty in calculating the different reservoir properties of the injection formations.

Table 3—Comparison between the Original Values and Generic Forms Values

Well Name	Original Values		Generic Forms Values	
	C_1	C_2	C_1	C_2
Reed	0.642	886.71	0.6173	887.24
A	0.5929	1061.6	0.6328	1083.26
B	0.7422	589.36	0.7413	642.86
C	0.2752	302.44	0.2763	301.23
D	0.6335	118.79	0.6173	130.15

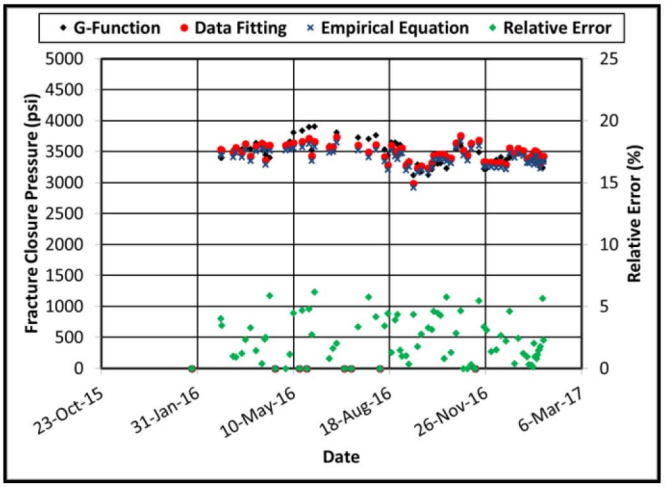

Figure 14—Comparing the Fracture Closure Pressure from the G-Function Analysis and from the New Emirical Equation for Reed We

Validating the New Technique (Case Studies)

Case Study (1): Repetto Sand, California, USA

Well SFI#3 is a biosolids injector which is used to inject treated solids and sludges from municipal waste water treatement operations into the Repetto Sand with the following properties:

Perforation top depth= 4959 ft

Porosity= 22 %

Permeability= 110 mD

Poisson's ratio= 0.33
Young's modulus= 1.5 Mpsi
Pore Pressure= 1977 psi

The ISIP was picked manually from the bottomhole pressure curve (3685 psi) as shown in (Fig. 15). On the other hand, the fracture closure pressure was determined using G-function analysis with a value of 2620 psi as shown in (Fig. 16).

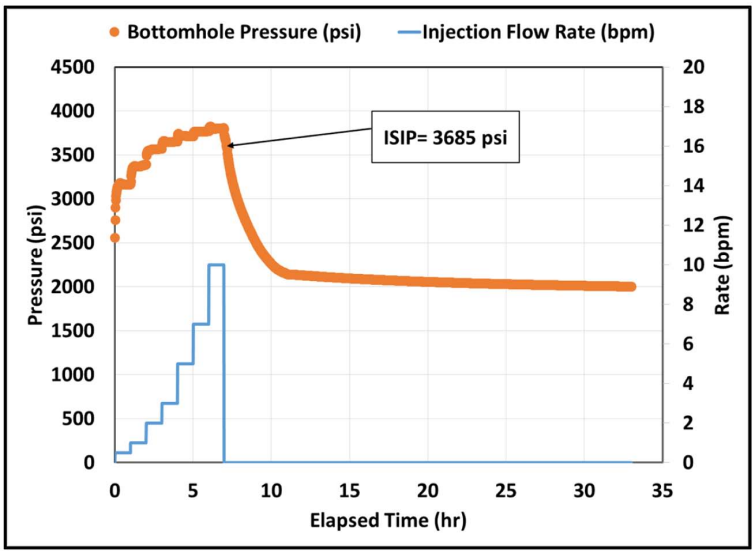

Figure 15—Injection Pressure and Injection Flow Rate Data for SFI#3

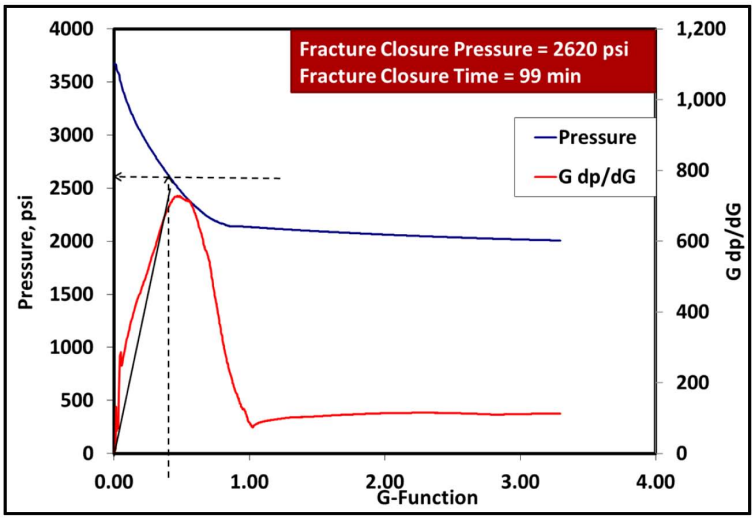

Figure 16—Fracture Closure Pressure from G-Function Analysis for SFI#3

The developed generic forms were used to calculate C_1 and C2 Coefficients resulted in the following:

C_1= 0.4933

C_2= 842.07

The fracture closure pressure was calculated as 2660 psi using Eq. 6 which is very close (1.5% difference) to the value obtained from the G-function analysis (2620 psi).

Case Study (2): Vaca Muerta Shale, Argentina (SPE 174380)
The Vaca Muerta shale is a gas bearing formation in Argentina. A mini-frac test was conducted in order to determine the fracture pressure and the formation permeability (Leak-off Coefficient) so that a fracture stimulation schedule could be designed later. The formation properties are lited below:

Vaca Muerta Properties:
Porosity= 11%
Pore pressure= 7600 psi
Perforation top depth= 9100 ft
Young's modulus= 1.4 Mpsi
Poisson's ratio= 0.22

Conventional Mini-frac test results are:
ISIP= 8482 psi
P_c= 8270 psi
K= 0.0009 mD

The empirical equation results are listed below:
C_1= 0.834
C_2= 1209.896
P_c= 8286 psi
The fracture closure pressure was calculated as 8286 psi using Eq. 6 as compared to 8270 obtained from the G-function analysis (0.19% difference).

Case Study (3): Tight Gas Sand (SPE 179725-PA)
Diagnostic fracture injection test (DFIT) was conducted on a gas bearing tight sand formation with the following properties:
Porosity= 0.16
Permeability= 0.00015 mD
Pore pressure= 4485 psi
Overburden pressure= 9967 psi
Poisson's ratio= 0.18
Young's modulus= 4.6 Mpsi

DFIT results:
ISIP= 8282
psi Pc= 7876 psi

The empirical equation results:
C_1= 0.834
C_2= 1212.618
Pc= 8122 psi
The empirical equation predicts the fracture closure pressure to be 8122 psi with a relative error of ~3.13% compared to the results that was obtained by DFIT analysis of 7876 psi.

Limitations

The new technique has limitations in terms of the rock properties to be used by the user as the empirical correlations were built using the following ranges:

Permeability 30-180 mD
Porosity 17-22 %
Young's Modulus 0.49-2.4 Mpsi
Poisson's Ratio 0.22-0.33

However, it might give acceptable results for low permeability formations in the micro-Darcy scale as discussed in case studies (2) and (3).

Conclusions

1. The new empirical equation predicts the fracture closure pressure from ISIP based on good knowledge of formation properties, i.e. Young's Modulus, Poisson's ratio, pore pressure, overburden pressure, porosity, and permeability.
2. The new empirical equation is a fast technique that can estimate the fracture closure pressure even before the fracture actually closes off. Therefore, the use of this technique is especially beneficial in cases of injection in highly damaged or low permeability formations where long periods of time, often up to several days, are required to collect the pressure falloff data until fracture closure is observed.
3. Future work is required to further assess the effects of varying injection volumes and injectant viscosity on the empirical equations in order to predict fracture closure pressure with a better accuracy espically for very tight sands and unconventional shale formations.

Nomenclature

D:	depth, ft
D_i:	equivalent depth of lowermost normally pressured formation, ft
K_i:	matrix stress coefficient
P_w:	wellbore pressure, psi
P:	formation pore pressure, psi
S:	overburden stress, psi
R:	resistivity, ohm-m
ρ_B:	average bulk density of sediments, gm/cc
Pc:	fracture closure pressure, psi
t:	elapsed time
t_p:	pumping duration
ISIP:	instantaneous shut-in pressure, psi
C_1, C_2:	linear correlation coefficients
q:	injection flow rate, bbl/day
B:	formation volume factor
μ:	formation fluid viscosity, cP
h:	formation thickness, ft
m':	horizontal level of the pressure derivative
K:	formation permeability, mD
Es:	static Young's modulus, GPa
Ed:	dynamic Young's modulus, GPa
v:	Poisson's ratio
Vp:	compressional wave velocity, Km/sec
Vs:	shear wave velocity, Km/sec
E:	Young's modulus, psi
σ:	net effective overburden stress, psi

g: acceleration of gravity, cm/sec^2
go: dimensionless loss volume function when t=t_p
Δt: sonic travel time, microsec/ft
Φ: porosity, fraction

Unit Conversion

Mpsi = 0.145 *GPa*

Km/sec = $\frac{305.4}{\mu sec/ft}$

References

Warpinski, N.R., and Branagan, P.T. (1989, Sptember 1). Altered Stress Fracturing. *Journal of Petroleum Technology.* **41** (09): 990–997. SPE-17533-PA

Perkins, T.K., and Gonzalez, J.A. (1985, February 1). The Effect of Thermoelastic Stresses on Injection Well Fracturing. *SPE Journal*. **25** (01): 78–88. SPE-11332-PA

Moschovidis, Z., Steiger, R., Weng, X., Frankl, M., Abou-Sayed, A. 1999. The Mounds Drill Cuttings Injection Field Experiment. Paper presented at the 37th US rock mechanics symposium, Vail, Colorado, USA, 7-9 June. ARMA 99-1017

Tiner, R.L., Ely, J.W., and Schraufnagel, R. 1996. Frac Packs-State of the Art. Paper presented at the SPE Annual Technical Conference and Exhibition, Denver, Colorado, USA, 6-9 October. SPE- 36456-MS

Barree, R.D., Barree, V.L., and Craig, D.P. (2009, August 1). Holistic Fracture Diagnostics: Consistent Interpretation of Prefrac Injection Tests Using Multiple Analysis Methods. *SPE Production & Operations* **24** (03): 396–406. SPE-107877-PA

Mohamed, I.M., Nasralla, R.A., Sayed M.A., Marongiu-Porcu, M., and Ehling-Economides, C.A. 2011. Evaluation of After Closure Analysis Techniques for Tight and Shale Gas Formations. Paper presented at the SPE Hydraulic Fracturing Technology Conference, The Woodlands, Texas, USA, 24-25 January. SPE-140136-MS

Gandossi, L., and Van Estorff, U. 2015. An Overview of Hydraulic Fracturing and other Formation Stimulation Technologies for Shale Gas Production. *Scientific and Policy Report by the Joint Research Centre of the European Commission*

Singh, P.K., Agarwal, R.G., and Krase, L.D. 1987. Systematic Design and Analysis of Step-Rate Tests to Determine Formation Parting Pressure. Paper presented at the SPE Annual Technical Conference and Exhibition, Dallas, Texas, USA, 27–30 September. SPE-16798-MS

Felsenthal, M. (1974, October 28). Step-Rate Tests Determine Safe Injection Pressures in Floods. *Oil and Gas Journal* **72** (43): 49–54

Nolte, K.G. (1988, February 1). Application of Fracture Design Based on Pressure Analysis. *SPE Production Engineering* **3** (01): 31–42. SPE-13393-PA

Nolte, K.G. 1979. Determination of Fracture Parameters from Fracturing Pressure Decline. Paper presented at the SPE Annual Technical Conference and Exhibition, Las Vegas, Nevada, USA, 23-26 September. SPE-8341-MS

Howard, G. C, Fast, C. R, and Carter R.D. 1957. Derivation of the General Equation for Estimation the Extent of the Fracture Area. *API Drilling and Production Practices*. 261–268. NY

Matthews, W. R., and Kelly, J. 1967. How to Predict Formation Pressure and Fracture Gradient. *Oil and Gas Journal* **65** (08): 92–106

HubbertM. K.,, and Willis.D.G., 1957. Mechanics of Hydraulic Fracturing. *AIME Petroleum Transactions* **210**: 153–168 SPE-686-G

Eaton, B.A. (1969, October 1). Fracture Gradient Prediction and its Application in Oilfield Operations. *SPE Journal of Petroleum Technology* **21** (10):1353–1360. SPE-2163-PA

Kiel, O.M. (1970, January 1). A New Hydraulic Fracturing Process. *Journal of Petroleum Technology* **22** (01): 89–96. SPE-2453-PA

Abou-Sayed, A.S., Andrews, D.E., and Buhidma, I.M. 1989. Evaluation of Oil Waste Injection below the Permafrost in Prudhoe Bay Field. Paper presented at the SPE California Regional Meeting, Bakersfield, California, USA, 5-7 April. SPE-18757-MS

Sirevag, G., and Bale, A. 1993. An Improved Method for Grinding and Reinjecting of Drill Cuttings. Presented at the SPE/IADC Drilling Conference, Amsterdam, The Netherlands, 22–25 February. SPE-25758-MS

Eaton, B.A.1975. The Equation for Geopressure Prediction from Well Logs. Paper presented at the SPE Fall Meeting, Dallas, Texas, USA, 28 September-1 October. SPE-5544-MS

Smolen, J.J., and Litsey, L.R. (1979, January 1). Formation Evaluation using Wireline Formation Tester Pressure Data. *Journal of Petroleum Technology* **31** (01): 25–32. SPE-6822-PA

Canady, W. 2011. A Method for Full-Range Young's Modulus Correction. Paper presented at the SPE North American Unconventional Gas Conference and Exhibition, The Woodlands, Texas, USA, 14-16 June. SPE-143604-MS

Coates, G.R., and Denoo, S.A. 1980. Log Derived Mechanical Properties and Rock Stress. Paper presented at the SPWLA 21st Annual Logging Symposium, Lafayette, Louisiana, USA, 8-11 July. SPWLA-1980-U

Horner, D.R.1951. Pressure Build-Up in Wells. Paper presented at the 3rd World Petroleum Congress, The Hague, The Netherlands, 28 May-6 June. WPC-4135

Bai, M, Diaz, A., Mclennan, J., and Reyna, J. 2013. Importance of Fracture Closure to Cuttings Injection Efficiency. Paper presented at the ISRM International Conference for Effective and Sustainable Hydraulic Fracturing, Brisbane, Australia, 20-22 May. ISRM-ICHF-2013-004

Warembourg, P.A., Klingensmith, E.A., HodgesJ.E.Jr,, and Erdle, J.E. 1985. Fracture Stimulation Design and Evaluation. Paper presented at the SPE Annual Technical Conference and Exhibition, Las Vegas, Nevada, USA, 22-26 September. SPE-14379-MS

Rohmer, B., Raverta, M., Boutaud de la Combe, J-L., and Jaffrezic, V. 2015. Minifrac Analysis using Well Test Technique as Applied to the Vaca Muerta Shale Play. Paper presented at the EUROPEC 2015, Madrid, Spain, 1–4 June, SPE-174380-MS

Buie, R.P-Jr., and Dang Y.H. 2000. Fracture Containment Mechanisms in Soft Rock Frac-Packs. Paper presented at the SPE International Symposium on Formation Damage Control, Lafayette, Louisiana, USA, 23–24 February. SPE-58763-MS

McClure, M.W., Jung, H., Cramer, D.D., and Sharma, M.M. (2016, August 1). The Fracture-Compliance Method for Picking Closure Pressure from Diagnostic Fracture Injection Tests. *SPE Journal* **21** (04): 1321–1339. SPE-179725-PA

Mclennan, J.D., and Roegiers, J.C. 1982. How Instantaneous are Instantaneous Shut-In Pressures. Paper presented at the SPE Annual Technical Conference and Exhibition, New Orleans, Louisiana, USA, 26-29 September. SPE-11064-MS

Howard, G.C., and Fast, C.R. (1970, February 1). Hydraulic Fracturing. *Monograph Volume 2 of the Henry L. Doherty Series*